Postfach 10 11 61
69451 Weinheim
Germany
Courier services:
Boschstraße 12
69469 Weinheim
Germany
Tel.: (+49) 6201 606 235 / 432
Fax: (+49) 6201 606 500
E-mail: advmat@wiley-vch.de

Dear Author,

Please correct your galley proofs carefully and return them no more than three days after the page proofs have been received.

If you have not used the PXE system before, please view the Tutorial before checking your proofs: http://wileypxe.aptaracorp.com/pxewileyvch/UserDocument/UserGuide/WileyPXE5_AuthorInstructions.pdf

Please note any queries that require your attention. These are indicated with red Qs in the pdf or highlighted as yellow queries in the "Edit" window.

Please pay particular close attention to the following, as no further corrections can be made once the article is published online:

- **Names** of all authors present and spelled correctly
- **Titles** of authors are correct (Prof. or Dr. only: please note, Prof. Dr. is not used in the journals)
- **Addresses of all authors** and **e-mail address of the corresponding author** are correct and up-to-date
- **Funding bodies** have been included and grant numbers are accurate
- The **Title** of the article is OK
- All **figures** are correctly included
- **Equations** are typeset correctly

Note that figure resolution in the PXE system is deliberately lower to reduce loading times. This will be optimized before the article is published online.

Please send any additional information, such as figures or other display items, to advmat@wiley-vch.de, and please also indicate this clearly in the PXE "Edit" window by inserting a comment using the query tool.

Reprints may be ordered by filling out the accompanying form.
Return the reprint order form by e-mail with the corrected proofs, to Wiley- VCH: **advmat@wiley-vch.de**

Please limit corrections to errors already in the text. Costs incurred for any further changes will be charged to the author, unless such changes have been agreed upon by the editor.

The editors reserve the right to publish your article without your corrections if the proofs do not arrive in time. Note that the author is liable for damages arising from incorrect statements, including misprints.

ADVANCED MATERIALS

Reprint Order Form 2017
- please return with your proofs -

Editorial Office:

Wiley-VCH Verlag, Boschstrasse 12
69469 Weinheim, Germany

Tel.: (+49) 6201 606 235
Fax: (+49) 6201 606 500

E-mail: advmat@wiley-vch.de
http://www.advmat.de

Manuscript No. _____

Please send me and bill me for

☐ no. of **reprints** via ☐ airmail (+ 25 Euro) ☐ surface mail

☐ no. of **copies of this issue** (1 copy: 25 Euro) via ☐ airmail (+ 25 Euro) ☐ surface mail

☐ **high-resolution PDF file** (330 Euro).
My e-mail address:

_____

Please note: It is not permitted to present the PDF file on the internet or on company homepages

★**Special Offer**★ If you order 200 or more reprints you will get a PDF file for half price.

Information regarding VAT
Please note that from German sales tax point of view, the charge for **Reprints, Issues or Posters** is considered as **"supply of goods"** and therefore, in general, such delivery is a subject to German sales tax. However, this regulation has no impact on customers located outside of the European Union. Deliveries to customers outside the Community are automatically tax-exempt. Deliveries within the Community to institutional customers outside of Germany are exempted from the German tax (VAT) only if the customer provides the supplier with his/her VAT number. The VAT number (value added tax identification number) is a tax registration number used in the countries of the European Union to identify corporate entities doing business there. It starts with a country code (e.g. FR for France, GB for Great Britain) and follows by numbers.

Mail reprints /cover posters / copies of the issue to:

_____
_____
_____
_____
_____

Invoice address:

_____
_____
_____
_____
_____

_____
Date, Signature **Stamp**

VAT no.: _____
(institutes / companies in EU countries only)

Purchase Order No.: _____

Credit Card Payment

VISA, MasterCard, AMERICAN EXPRESS
Please use the Credit Card Token Generator located at the website below to create a token for secure payment. The token will be used instead of your credit card number.

Credit Card Token Generator:
https://www.wiley-vch.de/editorial_production/index.php

Please transfer your token number to the space below.

Credit Card Token Number:

Cover Posters

Posters are available of all the published covers and frontispieces in two sizes

☐ DIN A2 42 x 60 cm / 17 x 24in (one copy: **39 Euro**)
☐ DIN A1 60 x 84 cm / 24 x 33in (one copy: **49 Euro**)

Postage for shipping posters overseas by airmail:
+ 25 Euro

Postage for shipping posters within Europe by surface mail:
+ 15 Euro

Price list for reprints (The prices include mailing and handling charges. All Wiley-VCH prices are exclusive of VAT)

No. of pages	Price (in Euro) for orders of 50 copies	100 copies	150 copies	200 copies	300 copies	500 copies
1-4	345	395	425	445	548	752
5-8	490	573	608	636	784	1077
9-12	640	739	786	824	1016	1396
13-16	780	900	958	1004	1237	1701
17-20	930	1070	1138	1196	1489	2022
for every additional 4 pages	147	169	175	188	231	315

★ **Special Offer** ★ If you order 200 or more reprints you will get a PDF file for half price.

Wiley-VCH Verlag GmbH & Co. KGaA; Location of the Company: Weinheim;
Chairman of the Supervisory Board: Stephen Michael Smith,
Trade Register: Mannheim, HRB 432833, General Partner: John Wiley & Sons GmbH,
Location: Weinheim, Trade Register Mannheim, HRB 432296,
Managing Director: Sabine Steinbach

WILEY-VCH

Communication

xxxx

H. Yao, L. Ye, J. Hou, B. Jang, G. Han, Y. Cui, G. M. Su, C. Wang, B. Gao, R. Yu, H. Zhang, Y. Yi,* H. Y. Woo,* H. Ade,* J. Hou* .....x–xx

Achieving Highly Efficient Nonfullerene Organic Solar Cells with Improved Intermolecular Interaction and Open-Circuit Voltage

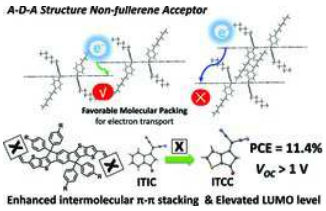

A new acceptor–donor–acceptor structured nonfullerene acceptor ITCC is designed and synthesized via simple end-group modification. ITCC shows improved electron transport properties and a high-lying lowest unoccupied molecular orbital level. A power conversion efficiency of 11.4% with an impressive V_{OC} of over 1 V is recorded in photovoltaic devices, suggesting great potential for applications in tandem organic solar cells.

adma201700254(201700254)

www.advmat.de ADVANCED MATERIALS

Achieving Highly Efficient Nonfullerene Organic Solar Cells with Improved Intermolecular Interaction and Open-Circuit Voltage

By *Huifeng Yao, Long Ye, Junxian Hou, Bomee Jang, Guangchao Han, Yong Cui, Gregory M. Su, Cheng Wang, Bowei Gao, Runnan Yu, Hao Zhang, Yuanping Yi,* Han Young Woo,* Harald Ade,* and Jianhui Hou**

ABSTRACT: A new acceptor–donor–acceptor structured nonfullerene acceptor ITCC is designed and synthesized via simple end-group modification. ITCC shows improved electron transport properties and a high-lying lowest unoccupied molecular orbital level. A power conversion efficiency of 11.4% with an impressive V_{OC} of over 1 V is recorded in photovoltaic devices, suggesting great potential for applications in tandem organic solar cells.

Q1

Organic solar cells (OSCs) with bulk heterojunction (BHJ) structures consisting of electron-donor and electron-acceptor materials have achieved impressive progress over the past decade,[1,2] demonstrating their great potential in practical applications. An efficient active layer must possess several features, including strong absorption over a broad range of the solar spectrum, proper alignment of molecular energy levels to allow for charge separation, high charge carrier mobility, and favorable blend morphology in the thin film.[3] All of these aspects play a role in dictating device performance, which is generally characterized by the short-circuit current density (J_{SC}), open-circuit voltage (V_{OC}), and fill factor (FF). In the past decades, research has focused on using fullerene derivatives as the electron acceptor in OSC devices. Furthermore, considerable efforts have been devoted to developing efficient molecular design strategies to optimize polymer or small-molecule (SM) electron donors,[4–7] with power conversion efficiencies (PCEs) of OSC devices based on fullerenes having surpassed 11%.[8] However, continued progress in fullerene-based OSCs is challenging, partly owing to their intrinsically large voltage losses (usually over 0.7 V),[9] defined as the difference between the optical bandgap of the active layer and the output voltage of the device.

The past few years have witnessed the rapid progress of nonfullerene acceptors, and the PCEs of nonfullerene-based OSC devices have been catching up and even surpassed that of their fullerene counterparts.[10–12] Compared to fullerenes, nonfullerene acceptors have some advantages such as greater tunability of the absorption spectra and molecular energy levels, potential for lower cost preparation and purification processes. Furthermore, it is worth noting that several studies have shown that the inevitable voltage losses are reduced in nonfullerene based OSCs,[13–15] which is beneficial for achieving high V_{OC} devices with outstanding photovoltaic performance. For example, when the electronic structure is tuned such that a V_{OC} reaches 1 V, devices based on fullerene acceptors can only yield relatively low PCEs of around 6%–7%[16,17] whereas nonfullerene-based OSCs can deliver PCEs of around 10%.[12,14] Over the past decade, many nonfullerene electron acceptors based on naphthalene diimide,[18] perylene diimide,[14,19–25] or indacenodithiophene (IDT)[13,15,26–29] units as core structures have been designed and applied to OSCs. Among these, SMs with an acceptor–donor–acceptor (A–D–A) structure such as ITIC,[27] IEIC,[26] and IDTBR,[30] have shown very good photovoltaic per-

H. Yao, Y. Cui, B. Gao, R. Yu, H. Zhang, Prof. J. Hou, Beijing National Laboratory for Molecular Sciences, State Key Laboratory of Polymer Physics and Chemistry, Institute of Chemistry, Chinese Academy of Sciences, Beijing, 100190, P. R. China

Q2

H. Yao, G. Han, Y. Cui, B. Gao, R. Yu, H. Zhang, Prof. Y. Yi, Prof. J. Hou, University of Chinese Academy of Sciences, Beijing, 100049, P. R. China

Dr. L. Ye, Prof. H. Ade, Department of Physics and Organic and Carbon Electronics Lab (ORaCEL), North Carolina State University, Raleigh, NC, 27695, USA

Dr. J. Hou, Department of Composite Materials and Engineering, College of Materials Science and Engineering, Hebei University of Engineering, Handan, 056038, P. R. China

B. Jang, Prof. H. Y. Woo, Department of Chemistry, Korea University, Seoul, 136-701, Republic of Korea

G. Han, Prof. Y. Yi, Beijing National Laboratory for Molecular Science, Key Laboratory of Organic Solids Institute of Chemistry, Chinese Academy of Sciences, Beijing, 100190, P. R. China

Dr. G. M. Su, Dr. C. Wang, Advanced Light Source, Lawrence Berkeley National Laboratory, Berkeley CA, 94720, USA

Correspondence to: Prof. Y. Yi (E-mail: ypyi@iccas.ac.cn), Prof. H. Y. Woo (E-mail: hywoo@korea.ac.kr), Prof. H. Ade (E-mail: hwade@ncsu.edu), Prof. J. Hou (E-mail: hjhzlz@iccas.ac.cn)

Q3

10.1002/adma.201700254

ADVANCED MATERIALS www.advmat.de

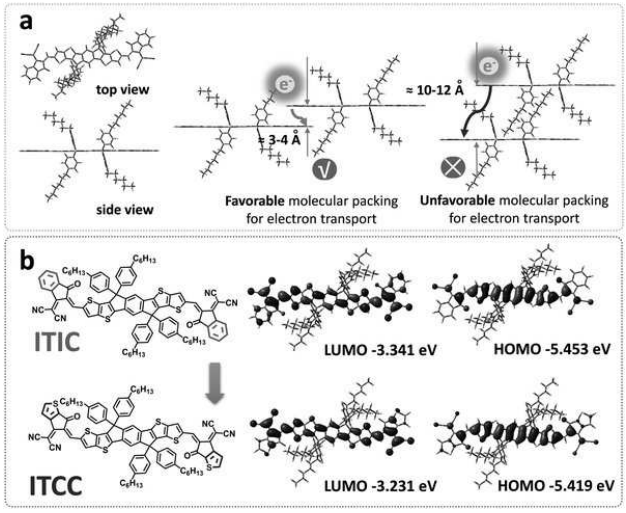

Figure 1. a) Schematic illustration of molecular stacking of the highly efficient A-D-A structured SM acceptor. b) Optimized molecular geometries and frontier molecular orbitals for ITIC and ITCC.

formance. For instance, as the first SM acceptor that breaks the 10% efficiency, ITIC has been widely studied and achieved many great successes. Although ITIC can work well with multiple polymer donors, the OSC devices only deliver relatively low V_{OC} (≈0.82–0.94 V)[9,27,31] because ITIC has a relatively low-lying lowest unoccupied molecular orbital (LUMO) level of −3.83 eV.[29] What's more, the electron mobility of ITIC (2.6×10^{-4} cm^2 V^{-1} s^{-1}) is still lower than of the fullerene-based acceptors, hence further improvement is required for efficient charge transfer in the devices.

From the aspect of molecular structure, the highly efficient A–D–A SMs all have large, branched side chains attached to the core units to provide solubility, which impedes the compact stacking of the core moieties of the molecules (**Figure 1**a). Therefore, the stacking of electron-withdrawing end-groups in this type of acceptor molecules may provide the main electron transport channels, determining overall electron transport properties. What's more, calculations based on density functional theory (DFT) reveal that the electron density distribution of the LUMO extends over the end-groups, but the electron density distribution of the highest occupied molecular orbital (HOMO) resides mostly on the central donor unit. This suggests that the properties of the LUMO could be easily tuned by end-groups modification, making end-group modification of this type of SM acceptor potentially a very important factor that could influence molecular packing and frontier orbital properties.

Here, we report the design and synthesis of a novel nonfullerene acceptor, ITCC (Figure 1b), which is based on introducing thienyl-fused indanone as end-groups on a previously reported SM acceptor ITIC. Due to enhanced intermolecular interactions, ITCC exhibits a closer π–π stacking distance compared to ITIC. Theoretical predictions and experimental results demonstrate that ITCC has improved charge transport properties relative to ITIC. In addition, the LUMO level of ITCC elevated by about 110 meV relative to ITIC. In OSC devices consisting of PBDB-T[32] as the polymer donor, ITCC-based OSC device obtains an impressive V_{OC} of greater than 1 V while ITIC-based device only yields a V_{OC} of 0.93 V. Morphology studies of the blend films imply that purer domains are formed in the ITCC-containing film than that of ITIC-containing film, and this could suppress bimolecular recombination in the devices. This contribution highlights the influence of end-group modification on the properties of an A–D–A SM acceptor. The high PCE of 11.4% suggests that ITCC is a promising acceptor candidate for efficient OSCs.

Since a sulfur atom is more easily polarized compared to a carbon atom due to its more loosely held electrons relative to a benzene ring, the thiophene-containing conjugated molecules usually have stronger intermolecular π–π interactions.[29] Hence, the thienyl-fused indanone end-groups of ITCC are expected to enhance intermolecular π–π interactions and facilitate charge transport compared to ITIC which contains phenyl-fused indanone end-groups. In addition, the more electron-donating nature of thiophene compared to benzene should result in an up-shifted LUMO for ITCC, which contains the thienyl-fused end-group, relative to ITIC. This increased LUMO can also help obtain a higher V_{OC}. Quantum chemical calculations were performed to help understand the rational design of new nonfullerene acceptors. As shown in Figure 1b, the optimized molecular conformations and wavefunction distributions of the frontier orbitals (determined using DFT at a B3LYP level of theory and a 6-31G(d,p) basis set) do not show much difference between ITIC and ITCC. Compared with ITIC, however, the calculated HOMO and LUMO levels of ITCC are simultaneously up-shifted by 34 and 110 meV, respectively, leading to an increased calculated optical bandgap for ITCC. Geometry optimization of isolated ITIC and ITCC molecules was performed by DFT-D (DFT including the D3 version of Grimme's dispersion[33] to accurately describe the weak interactions) and the long alkyl side chains were replaced by methyl groups to reduce the computation time. The optimized geometry of dimer molecules was used to evaluate the intermolecular interactions during intermolecular self-assembly (Figure S1, Supporting Information), and the intermolecular binding energies of ITIC and ITCC based on optimized dimers were calculated to be −24.06 and −26.65 Kcal mol^{-1}, respectively, under the correction of basis set superposition error (BSSE).[34] The decreased binding energy of ITCC by 2.59 Kcal mol^{-1} suggests that ITCC molecules have a stronger tendency for intermolecular stacking, which will enhance its crystalline properties and improve charge carrier mobility.

As presented in **Scheme 1**, ITCC was prepared from thiophene-2-carboxylic acid via a four-step process. First, acylchlorination of carboxylic acid was conducted using thionyl chloride as a chlorinating agent. After removing the solvent and excess reactant, the resulting compound 2 was used in the next step without further purification. Then, Friedel–Crafts reaction between compound 2 and malonyl dichloride catalyzed by aluminium trichloride yielded compound 3. The key intermediate, compound 4, was obtained by treating compound

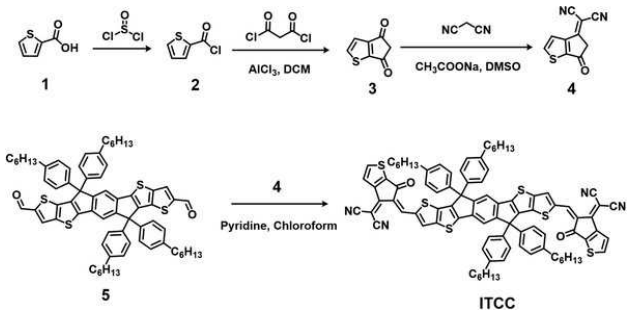

Scheme 1. Synthetic route of the SM acceptor ITCC.

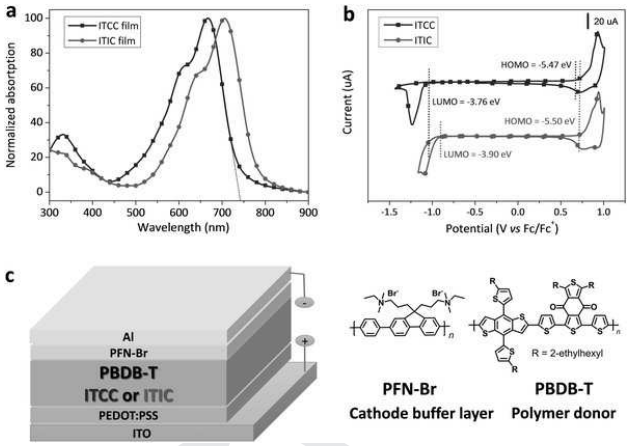

Figure 2. a) Normalized UV–vis absorption spectra of ITIC and ITCC thin films spin-coated from chloroform solution. b) CV plots of ITIC and ITCC measured in 0.1 M Bu_4NPF_6 acetonitrile solution at a scan rate of 50 mV s^{-1}. c) OSC device structure and molecular structures of the cathode buffer layer and the polymer donor.

3 with malononitrile using dimethylsulfoxide as a solvent at ambient temperature. Finally, the target product of ITCC was prepared by the Knoevenagel Condensation reaction between compound 4 and compound 5 in a high yield of 80% with the assistance of a microwave reactor. ITCC can be easily dissolved in common solvents like dichloromethane, chloroform, and chlorobenzene. The detailed synthetic procedures and characterizations of the intermediates are provided in the Experimental Section of the Supporting Information.

The normalized ultraviolet–visible (UV–Vis) absorption spectra of neat ITCC and ITIC thin films are presented in **Figure 2**a. In chloroform, the main absorption band of ITCC extends from 450 to 700 nm with a maximum absorption peak at 640 nm (Figure S2, Supporting Information). From solution to thin film, a red-shift by 30 nm was observed with an absorption onset at 742 nm, corresponding to an optical bandgap of 1.67 eV. Compared to ITIC ($E_g^{opt} = 1.59$ eV) thin films, the blue-shifted absorption spectrum of ITCC thin films (Figure 2a) can be attributed to the decreased intermolecular charge transfer (ICT) due to the more electron-donating thiophene units relative to benzene units, and less solar photons will be absorbed for the corresponding OSC devices. The frontier orbital levels of ITCC and ITIC were evaluated by cyclic voltammetry (CV) measurements to study the influence of introducing thiophene units, and ferrocene was used as an external standard in parallel. As shown in Figure 2b, relative to ITIC (HOMO = −5.50 eV, LUMO = −3.90 eV), the frontier orbital levels of ITCC are up-shifted, resulting in a HOMO of −5.47 eV and a LUMO of −3.76 eV. The greater change in the LUMO level (140 meV) compared to the HOMO level (30 meV) is consistent with the DFT results, and the high-lying LUMO level of ITCC is expected to increase the V_{OC} in photovoltaic devices.

The crystalline properties of ITIC and ITCC thin films were investigated by grazing-incidence wide-angle X-ray scattering (GIWAXS). As shown in Figure S3 in the Supporting Information, ITCC and ITIC films show (010) diffraction peaks in the out-of-plane (OOP) direction and a relatively uniform (100) signal, implying preferential face-on orientation of the crystallites. It is worth noting that the π–π stacking distance extracted from the peak location decreases slightly to 3.7 Å for ITCC from 3.8 Å for ITIC. This is in agreement with the enhanced intermolecular interactions predicted by DFT. The tight π–π stacking of ITCC molecules should help obtain a high electron mobility, and this is supported by space-charge-limited current (SCLC)[35] measurements (Figure S4, Supporting Information) which show the electron mobility of ITCC (9.26×10^{-4} cm^2 V^{-1} s^{-1}) is much higher than that of ITIC (1.76×10^{-4} cm^2 V^{-1} s^{-1}), which is favorable for the effective charge transport and extraction in the devices.

To investigate the photovoltaic performance of the newly designed SM acceptor, OSC devices with a conventional configuration of indium tin oxide/poly(3,4-ethylenedioxythiophene):poly(styrenesulfonate) (PEDOT:PSS)/active blend/poly[(9,9-bis(3′-((*N*,*N*-dimethyl)-*N*-ethylammonium)-propyl)-2,7-fluorene)-alt-2,7-fluorene)-alt-2,7-(9,9-dioctylfluorene)]dibromide (PFN-Br)[36]/Al (**Figure 2**c) were fabricated, in which the PEDOT:PSS and PFN-Br performed as the anode and cathode electrode buffer layers, respectively. Our previous publications have demonstrated that the polymer donor, PBDB-T[32] (Figure 2c), works well with A–D–A structured nonfullerene acceptors such as ITIC[10] and IT-M.[11] Therefore, we fabricated the OSC devices using PBDB-T as the polymer donor. After device optimization of donor:acceptor (D/A) weight ratio and solvent additive (Table S1, Supporting Information), we found the processing conditions of ITCC-based OSC devices are the same as for ITIC-based devices. As shown in the current density–voltage (*J*–*V*) curves (**Figure 3**a), the PBDB-T:ITCC device shows a maximum PCE of 11.4% with an impressive V_{OC} of 1.01 V, a J_{SC} of 15.9 mA cm^{-2} and a FF of 0.71. Meanwhile, the OSC device based on PBDB-T:ITIC shows a lower PCE of 10.6% with a V_{OC} of 0.93 V, a J_{SC} of 17.0 mA cm^{-2} and a FF of 0.67 under the same processing conditions and the same PBDB-T batch, which has some small differences (PCE over 11% could also be achieved with a higher FF but a relatively low V_{OC}) when inverted device structure was adopted in our previous work.[10] The enhancement of V_{OC} for the ITCC-based devices can be attributed to the up-shifted LUMO level of ITCC, and

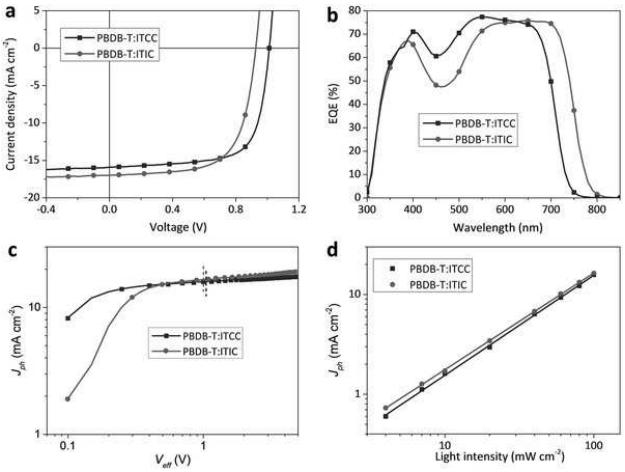

Figure 3. a) *J–V* and b) EQE curves for the devices based on ITIC and ITCC. c) Photocurrent dependences on the effective voltage and d) light intensity for the ITIC- and ITCC-based OSC devices.

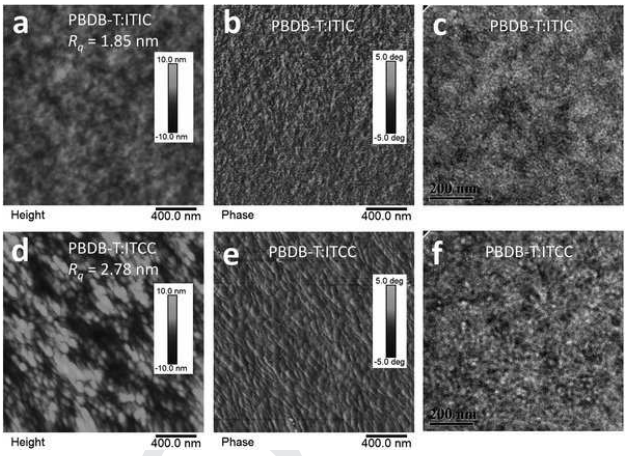

Figure 4. a) AFM height, b) AFM phase, and c) TEM images of the PBDB-T:ITIC blend film. d) AFM height, e) AFM phase, and f) TEM images of the PBDB-T:ITCC blend film.

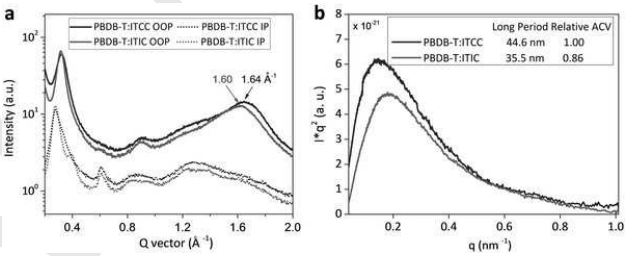

Figure 5. a) The OOP (solid line) and IP (dotted line) line-cut profiles of GIWAXS patterns of the blend films. b) Normalized and circularly averaged R-SoXS profiles of PBDB-T:ITIC and PBDB-T:ITCC blend films acquired at 283.8 eV.

a high efficiency over 11% with V_{OC} over 1 V has been rarely reported previously. Compared with the ITIC-based device, the slightly decreased J_{SC} of ITCC-based device at least in part due to its narrowed absorption band as discussed below. Then we fabricated ITIC- and ITCC-based OSC devices with different film thicknesses, and the results (Figure S5, Supporting Information) suggest PBDB-T:ITCC-based devices can keep ≈90% efficiency at a film thickness around 200 nm while the efficiency of PBDB-T:ITIC-based device drops to its ≈80%.[37]

The external quantum efficiency (EQE) curves of devices are demonstrated in Figure 3b. Compared to ITIC, ITCC-based device has a narrower photoresponse range. However, as the polymer donor PBDB-T and the small molecule acceptor ITCC all have absorption bands covering 450–750 nm, the device has very high EQE response in this region with a maximum value of 78% at 550 nm. The integrated current densities are 15.2 and 16.3 mA cm^{-2} for ITCC- and ITIC-based devices, respectively, which are consistent with the *J–V* measurements.

In order to investigate the origin for the improved FF in the ITCC-based devices, we conducted photocurrent analysis and characterized blend film morphology. Figure 3c shows the photocurrent dependence on effective voltage (V_{eff}) of the devices,[38] from which the J_{ph}/J_{sat} (J_{ph} is defined as the difference between the light current and dark current, J_{sat} represents the saturation current) ratios under short-circuit conditions and is calculated to be 0.90 and 0.87 for ITCC- and ITIC-based OSC devices, implying the overall exciton dissociation and charge collection processes all are quite efficient. Fitting the relationship of photocurrent and light intensity,[39] as shown in Figure 3d, the power-law exponents of the equation $J_{ph} \propto P_{light}^{s}$ for the ITCC- and ITIC-based devices are 1.00 and 0.96, respectively, suggesting that the bimolecular recombination is more efficiently suppressed in the ITCC-based device. The hole and electron mobilities of the blends were also measured by using SCLC method (Figure S6, Supporting Information). PBDB-T:ITCC blend has a higher electron mobility (6.74×10^{-4} cm^2 V^{-1} s^{-1}) than PBDB-T:ITIC blend (1.28×10^{-4} cm^2 V^{-1} s^{-1}) while they have similar hole mobilities.

The surface and bulk morphology of the blend films were first studied by atomic force microscopy (AFM) and transmission electron microscopy (TEM). As displayed in **Figure 4**, the AFM height images reveal that the root-mean-square surface roughness (R_q) of the PBDB-T:ITCC blend film is greater (2.78 nm) compared to PBDB-T:ITIC blends (1.85 nm), and larger aggregation domains were observed in the phase image. The TEM images also confirm the larger domains in the bulk of the PBDB-T:ITCC blend film, which may be attributed to the stronger intermolecular interactions of ITCC and thus stronger aggregation during casting.

In order to gain a deeper understanding about the influence of morphology on the device performance, we conducted GIWAXS and resonant soft X-ray scattering (R-SoXS) measurements on the blend films, from which the detailed morphology information such as molecular packing/orientation, domain length scales, and average composition variation (ACV) in blend films can be extracted. From the 2D-GIWAXS patterns (Figure S7, Supporting Information), we can find that both of the blend films display strong π–π stacking (010) scattering in

the OOP direction. Although the (010) peak positions of the polymer donor and the SM acceptors have some overlap (**Figure 5**a), the q values are 1.60 and 1.64 Å^{-1} for PBDB-T:ITIC and PBDB-T:ITCC blend films, respectively, corresponding to π–π stacking distances of 3.93 and 3.83 Å. The smaller (010) stacking distance of PBDB-T:ITCC blend film could be a result of enhanced intermolecular interactions of ITCC molecules, which is favorable for charge transport in the OSC device.

Having determined the molecular packing by GIWAXS, we employed R-SoXS to gain insight into the origin of the device performance. Taking advantage of the excellent material contrast over vacuum contrast in the soft X-ray regime (Figure S8, Supporting Information), R-SoXS allows a quantitative determination of key morphological parameters such as domain length scales and ACV in organic thin films for solar cell applications.[40] Figure 5b displays the 1D scattering profiles of both blend films acquired at 283.8 eV and normalized to thickness and absorption. It is noteworthy to mention that both R-SoXS profiles are completely dominated by a single log-normal distribution, indicative of a single length scale of phase separation (Figure S9, Supporting Information). The peak position represents the characteristic mode length scale (long period) of the blend film. We found the scattering maximum of the blend shifts toward lower q when replacing ITIC with ITCC as an acceptor material. As the ACV is proportional to the root square of the integrated scattering intensity (ISI, ISI $= \int I(q)q^2\mathrm{d}q$) over the full q range probed,[11,41] it can reflect the average purity of the mixed domains. Compared to the PBDB-T:ITIC film, the ITCC blend shows a higher relative ACV (1.00 vs 0.86). This purer domain suppresses the bimolecular recombination and thus contributes to a higher FF of 71% in the PBDB-T:ITCC device. Such a strong correlation between FF and ACV is also consistent with our recent observations on other high-efficiency nonfullerene system,[11] and fullerene system.[42]

In conclusion, a novel SM acceptor with an A–D–A motif and thienyl-fused indanone end-groups, ITCC, was rationally designed and synthesized via an end-group modulation. ITCC shows a closer π–π stacking distance and a higher electron mobility compared to ITIC, which contains phenyl-fused indanone end-groups. In addition, ITCC possesses a higher lying LUMO level of −3.76 eV and thus yields a V_{OC} of greater than 1 V in photovoltaic devices. The PCE of 11.4% demonstrates that the high V_{OC} nonfullerene OSC has a great potential for further improvement of efficiency. However, due to the blue-shifted optical absorption of ITCC, the J_{SC} of ITCC-based OSC device is not very high. Predictably, if both of the HOMO and LUMO energy levels of the nonfullerene acceptor can be up-shifted simultaneously, improved V_{OC} along with high J_{SC} and thus further improvement of PCE can be expected. The morphology study of the blend films suggests that the ITCC system may be an ideal model system with high V_{OC} to map out morphology evolution and its impact in nonfullerene solar cells.

Supporting Information

Supporting Information is available from the Wiley Online Library or from the author.

Acknowledgements

The authors acknowledge the financial support from the Ministry of Science and Technology of China (2014CB643501), NSFC (21325419, 91333204, 51373181), the Chinese Academy of Science (XDB12030200, KJZD-EW-J01), the CAS-Croucher Funding Scheme for Joint Labs (CAS14601). NEXAFS and R-SoXS data analyses by L.Y. and H.A. were supported by the ONR grant N00141512322. X-ray data were acquired at beamlines 11.0.1.2, and 5.3.2.2 at the Advanced Light Source, which was supported by the Director, Office of Science, Office of Basic Energy Sciences, of the U.S. Department of Energy under Contract No. DE-AC02-05CH11231. A. L. D. Kilcoyne, Y. Yu, and A. Young of the ALS (LBNL) provided instrument maintenance. H.Y. Woo acknowledges the financial support from National Research Foundation (NRF) of Korea (2012M3A6A7055540).

Received: January 12, 2017
Revised: February 21, 2017
Published Online: MM DD, YYYY

[1] A. J. Heeger, *Adv. Mater.* **2014**, *26*, 10.
[2] G. Li, R. Zhu, Y. Yang, *Nat. Photonics* **2012**, *6*, 153.
[3] Y. F. Li, *Acc. Chem. Res.* **2012**, *45*, 723.
[4] H. Yao, L. Ye, H. Zhang, S. Li, S. Zhang, J. Hou, *Chem. Rev.* **2016**, *116*, 7397.
[5] C. Duan, F. Huang, Y. Cao, *J. Mater. Chem.* **2012**, *22*, 10416.
[6] P. M. Beaujuge, J. M. J. Fréchet, *J. Am. Chem. Soc.* **2011**, *133*, 20009.
[7] Z. B. Henson, K. Mullen, G. C. Bazan, *Nat. Chem.* **2012**, *4*, 699.
[8] J. Zhao, Y. Li, G. Yang, K. Jiang, H. Lin, H. Ade, W. Ma, H. Yan, *Nat. Energy* **2016**, *1*, 15027.
[9] H. Bin, L. Gao, Z. G. Zhang, Y. Yang, Y. Zhang, C. Zhang, S. Chen, L. Xue, C. Yang, M. Xiao, Y. Li, *Nat. Commun.* **2016**, *7*, 13651.
[10] W. Zhao, D. Qian, S. Zhang, S. Li, O. Inganas, F. Gao, J. Hou, *Adv. Mater.* **2016**, *28*, 4734.
[11] S. Li, L. Ye, W. Zhao, S. Zhang, S. Mukherjee, H. Ade, J. Hou, *Adv. Mater.* **2016**, *28*, 9423.
[12] D. Baran, R. S. Ashraf, D. A. Hanifi, M. Abdelsamie, N. Gasparini, J. A. Rohr, S. Holliday, A. Wadsworth, S. Lockett, M. Neophytou, C. J. Emmott, J. Nelson, C. J. Brabec, A. Amassian, A. Salleo, T. Kirchartz, J. R. Durrant, I. McCulloch, *Nat. Mater.* **2016**, DOI: 10.1038/nmat4797. Q5
[13] H. Bin, Z. G. Zhang, L. Gao, S. Chen, L. Zhong, L. Xue, C. Yang, Y. Li, *J. Am. Chem. Soc.* **2016**, *138*, 4657.
[14] J. Liu, S. Chen, D. Qian, B. Gautam, G. Yang, J. Zhao, J. Bergqvist, F. Zhang, W. Ma, H. Ade, O. Inganäs, K. Gundogdu, F. Gao, H. Yan, *Nat. Energy* **2016**, *1*, 16089.
[15] H. Yao, Y. Chen, Y. Qin, R. Yu, Y. Cui, B. Yang, S. Li, K. Zhang, J. Hou, *Adv. Mater.* **2016**, *28*, 8283.
[16] J. Yuan, Z. Zhai, H. Dong, J. Li, Z. Jiang, Y. Li, W. Ma, *Adv. Funct. Mater.* **2013**, *23*, 885.

ADVANCED MATERIALS www.advmat.de

Table 1. Summary of photovoltaic parameters of the ITCC- and ITIC-based OSCs under simulated AM 1.5 G (100 mW cm^{-2}) illumination.

Device	V_{OC} [V]	J_{SC}[a)] [mA cm^{-2}]	FF	PCE[b)] [%]
PBDB-T:ITCC	1.01	15.9 (15.2)	0.71	11.4 (11.0)
PBDB-T:ITIC	0.93	17.0 (16.3)	0.67	10.6 (10.3)

[a)] Integrated current density from EQE spectrum; [b)] Average PCE values obtained from 10 devices are shown in parentheses.

[17] J. Warnan, C. Cabanetos, R. Bude, A. El Labban, L. Li, P. M. Beaujuge, *Chem. Mater.* **2014**, *26*, 2829.
[18] L. Ye, X. Jiao, M. Zhou, S. Zhang, H. Yao, W. Zhao, A. Xia, H. Ade, J. Hou, *Adv. Mater.* **2015**, *27*, 6046.
[19] Y. Zang, C.-Z. Li, C.-C. Chueh, S. T. Williams, W. Jiang, Z.-H. Wang, J.-S. Yu, A. K. Y. Jen, *Adv. Mater.* **2014**, *26*, 5708.
[20] Y. Zhong, M. T. Trinh, R. Chen, W. Wang, P. P. Khlyabich, B. Kumar, Q. Xu, C.-Y. Nam, M. Y. Sfeir, C. Black, M. L. Steigerwald, Y.-L. Loo, S. Xiao, F. Ng, X. Y. Zhu, C. Nuckolls, *J. Am. Chem. Soc.* **2014**, *136*, 15215.
[21] D. Sun, D. Meng, Y. Cai, B. Fan, Y. Li, W. Jiang, L. Huo, Y. Sun, Z. Wang, *J. Am. Chem. Soc.* **2015**, *137*, 11156.
[22] C.-H. Wu, C.-C. Chueh, Y.-Y. Xi, H.-L. Zhong, G.-P. Gao, Z.-H. Wang, L. D. Pozzo, T.-C. Wen, A. K. Y. Jen, *Adv. Funct. Mater.* **2015**, *25*, 5326.
[23] O. K. Kwon, J.-H. Park, D. W. Kim, S. K. Park, S. Y. Park, *Adv. Mater.* **2015**, *27*, 1951.
[24] J. Zhao, Y. Li, H. Lin, Y. Liu, K. Jiang, C. Mu, T. Ma, J. Y. Lin Lai, H. Hu, D. Yu, H. Yan, *Energy Environ. Sci.* **2015**, *8*, 520.
[25] D. Meng, D. Sun, C. Zhong, T. Liu, B. Fan, L. Huo, Y. Li, W. Jiang, H. Choi, T. Kim, J. Y. Kim, Y. Sun, Z. Wang, A. J. Heeger, *J. Am. Chem. Soc.* **2016**, *138*, 375.
[26] Y. Lin, Z.-G. Zhang, H. Bai, J. Wang, Y. Yao, Y. Li, D. Zhu, X. Zhan, *Energy Environ. Sci.* **2015**, *8*, 610.
[27] Y. Lin, J. Wang, Z.-G. Zhang, H. Bai, Y. Li, D. Zhu, X. Zhan, *Adv. Mater.* **2015**, *27*, 1170.
[28] Y. Lin, Q. He, F. Zhao, L. Huo, J. Mai, X. Lu, C. J. Su, T. Li, J. Wang, J. Zhu, Y. Sun, C. Wang, X. Zhan, *J. Am. Chem. Soc.* **2016**, *138*, 2973.
[29] Y. Lin, F. Zhao, Q. He, L. Huo, Y. Wu, T. C. Parker, W. Ma, Y. Sun, C. Wang, D. Zhu, A. J. Heeger, S. R. Marder, X. Zhan, *J. Am. Chem. Soc.* **2016**, *138*, 4955.
[30] D. Baran, T. Kirchartz, S. Wheeler, S. Dimitrov, M. Abdelsamie, J. Gorman, R. S. Ashraf, S. Holliday, A. Wadsworth, N. Gasparini, P. Kaienburg, H. Yan, A. Amassian, C. J. Brabec, J. R. Durrant, I. McCulloch, *Energy Environ. Sci.* **2016**, DOI: 10.1039/C6EE02598F.
[31] Z. Li, K. Jiang, G. Yang, J. Y. L. Lai, T. Ma, J. Zhao, W. Ma, H. Yan, *Nat. Commun.* **2016**, *7*, 13094.
[32] D. Qian, L. Ye, M. Zhang, Y. Liang, L. Li, Y. Huang, X. Guo, S. Zhang, Z. a. Tan, J. Hou, *Macromolecules* **2012**, *45*, 9611.
[33] S. Grimme, J. Antony, S. Ehrlich, H. Krieg, *J. Chem. Phys.* **2010**, *132*, 154104.
[34] S. l. Simon, M. Duran, J. J. Dannenberg, *J. Chem. Phys.* **1996**, *105*, 11024.
[35] A. Rose, *Phys. Rev.* **1955**, *97*, 1538.
[36] T. B. Yang, M. Wang, C. H. Duan, X. W. Hu, L. Huang, J. B. Peng, F. Huang, X. Gong, *Energy Environ. Sci.* **2012**, *5*, 8208.
[37] A. Armin, J. Subbiah, M. Stolterfoht, S. Shoaee, Z. Xiao, S. Lu, D. J. Jones, P. Meredith, *Adv. Energy Mater.* **2016**, *6*, 1600939.
[38] H. Lin, S. Chen, Z. Li, J. Y. Lai, G. Yang, T. McAfee, K. Jiang, Y. Li, Y. Liu, H. Hu, J. Zhao, W. Ma, H. Ade, H. Yan, *Adv. Mater.* **2015**, *27*, 7299.
[39] Y.-J. Hwang, H. Li, B. A. E. Courtright, S. Subramaniyan, S. A. Jenekhe, *Adv. Mater.* **2016**, *28*, 124.
[40] J. H. Carpenter, A. Hunt, H. Ade, *J. Electron Spectrosc.* **2015**, *200*, 2.
[41] S. Mukherjee, X. Jiao, H. Ade, *Adv. Energy Mater.* **2016**, *6*, 1600699.
[42] S. Mukherjee, C. M. Proctor, J. R. Tumbleston, G. C. Bazan, T.-Q. Nguyen, H. Ade, *Adv. Mater.* **2015**, *27*, 1105.

Q1 APT to AU: Please define 'ITCC' at its first occurrence in the abstract, text, and TOC.
Q2 APT to AU: Please verify the affiliation of authors 'Junxian Hou' and 'Jianhui Hou'.
Q3 APT to AU: Please provide the highest academic title (either Dr. or Prof.) for all authors, where applicable.
Q4 APT to AU: The citation for Table 1 is missing in the main text. Please add a citation at the appropriate place.
Q5 APT to AU: Please provide volume and page number in refs. [12, 30] if now available.